Correlations of α-decay properties and isospin-asymmetry

W. M. Seif,[1] G. G. Adamian,[2] N. V. Antonenko,[2] and A. S. Hashem[1]
[1]*Department of Physics, Faculty of Science, Cairo University, 12613 Giza, Egypt*
[2]*Joint Institute for Nuclear Research, 141980 Dubna, Russia*

(Received 30 April 2021; accepted 13 July 2021; published 27 July 2021)

The isospin-asymmetry nuclear chains with $N-Z$ from 2 to 60 are investigated to find the correlations of α-decay properties and isospin asymmetry. Both the proton- and neutron-skin thicknesses of α emitters belonging to different $N-Z$ chains are tightly aligned along straight lines, the slope of which depends on the shell closure. For even-even α emitters, the neutron-skin thickness Δ_n multiplied by $N-Z$ is a parabolic function of the isospin-asymmetry parameter $I=(N-Z)/A$. For the nuclei of incomplete neutron shells, the α-decay half-life T_α exponentially increases with Δ_n in the isospin chain. In the nuclei with valence neutrons and/or protons outside the magic core, T_α exponentially decreases with increasing Δ_n. The values of T_α and Q_α are almost exponential functions of isospin asymmetry.

DOI: 10.1103/PhysRevC.104.014317

I. INTRODUCTION

The study of α decay has a long history. Its explanation was the first application of quantum theory. The success of this explanation predetermined the development of the methods to describe also cluster decays. In the microscopic consideration, the α-decay half-life T_α is inversely proportional to the product of spectroscopic factor and penetrability through the Coulomb barrier. These two values certainly depend on Q_α and nuclear structure. As a result, the known phenomenological expressions [1–10] for T_α mainly depend on Q_α and the charge Z of the mother nucleus, which are related to the threshold for α emission. These expressions contain several phenomenological parameters required to take into account the spectroscopic factor and peculiarities of the nucleus-nucleus interaction. The number of parameters is usually reduced if the spherical square well radius is used to define the size of the touching configuration consisting of α particle and daughter nucleus. The correlations between nuclear structure and α-decay mode have been confirmed in many studies, for example, in Refs. [11–17]. The knowledge of nuclear density distributions is necessary to calculate the interaction between α particle and mother nucleus as well as the spectroscopic factors.

The study of α decays improves our knowledge about the nature and properties of nuclear matter. The consideration of various correlations allows us to relate the formation of an α particle on the nuclear surface to the nuclear structure and to find some dependence of T_α on the nucleon-density profile, which can be useful for prediction of T_α for new isotopes. In Refs. [18–20], the correlation between T_α and neutron-skin thickness has been found. The α decay occurs easier at smaller neutron-skin thickness. Also, the difference of neutron-skin thicknesses in mother and daughter nuclei must be small. The smaller the difference of neutron-skin thickness, the smaller the value of T_α at the same Q_α values.

The isospin asymmetry of heavy and superheavy nuclei is one of the key quantities that determine their structure, stability, and fission barriers [16,21–23]. It affects their partial lifetimes against different decay modes such as α [16,22], β [23], and cluster decays [24]. In Fig. 1, the measured internal quadrupole momenta Q_2 of nuclei [25] with the same $N-Z$ value are shown as functions of mass number A. The nuclei with the same $N-Z$ form a chain where the nuclei differ by an α particle. As seen, in all these isospin chains of nuclei, the dependencies of Q_2 on A are similar regardless of the value of $N-Z$ and the starting nucleus with indicated Z. So, the isospin asymmetry plays an important role in establishing the correlations between the nuclear characteristics.

Generally, the isospin asymmetry of the involved nuclei impacts different stages of α and heavier cluster decays of heavy nuclei, starting from the preformation of the emitted light clusters in the surface region of parent nuclei and up to their penetrability [22]. Taking the nuclear isospin effects into account considerably improves the half-life and branching-ratio calculations [16,22,26,27]. It was found that, for α emitters with valence protons and neutrons outside closed shells, the preformation probability P_α of an α particle inside them increases upon increasing their isospin asymmetry coefficient I. If the shells in the parent nucleus require a few nucleons to be closed, the larger isospin asymmetry favors decreasing P_α. For given shell closures of an α emitter, P_α varies linearly with the isospin asymmetry parameter multiplied by the number of valence protons (N_p) and neutrons (N_n). These linear dependencies correlate with the closed shells core (Z_0, N_0). Similar individual linear behaviors were obtained as a function of N_pN_nI [22,28]. P_α was found to exhibit a nearly general linear trend as the function $N_pN_n/(Z_0+N_0)$ [22].

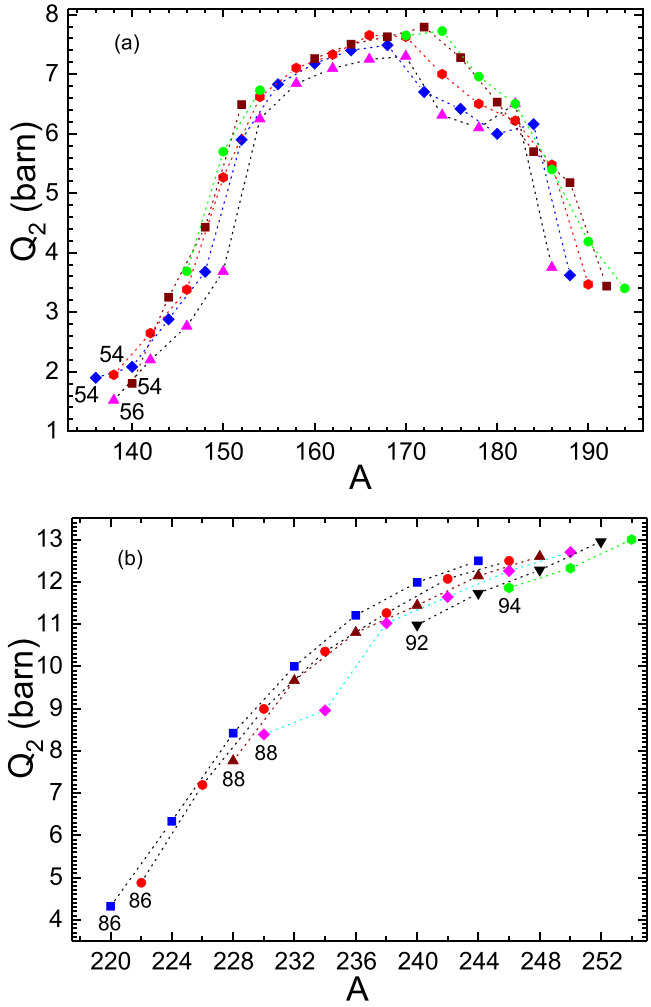

FIG. 1. (a) The internal quadrupole moment as a function of A for the isospin-asymmetry $(N-Z)$ chains stating from the nuclei with indicated charge numbers $50 < Z < 82$. (b) The same as in panel (a) but for nuclei with $Z > 82$. The data are taken from Ref. [25].

In the present paper, we use the self-consistent Skyrme Hartree-Fock-Bogoliubov (SHFB) calculations to find the neutron-skin thicknesses for many α emitters. Using these results, we study the correlations of neutron-skin thickness with T_α and isospin asymmetry $N-Z$. Knowing the correlations and establishing simple dependencies, one can predict T_α for new isotopes. Any correlations found can be useful to improve the energy-density functional and make simple estimates for presently unknown isotopes.

The paper is arranged as follows: In Sec. II, we outline the theoretical framework adopted for the mean-field calculations of the nuclear structure of the investigated nuclei, based on a Skyrme-like effective nucleon-nucleon force. The results and the experimental values for the even-even nuclei belonging to the investigated isospin-asymmetry chains are presented and discussed in Sec. III. Finally, we give brief conclusions in Sec. IV.

II. THEORETICAL FRAMEWORK

The self-consistent SHFB model is a successful nonrelativistic method which is widely used to investigate the nuclear structure and low-energy dynamics [29]. Because the SHFB equations are nonlinear in the wave functions [30], the mean-field and pairing field are self-consistently computed to obtain an optimized iterative solution [29]. In this method, the total energy of the nuclear system is expressed as a sum of the kinetic $H_{\rm kin}$, Skyrme H_{Sk}, Coulomb H_C, and pairing energy $H_{\rm Pair}$ terms, in addition to the correction term $E_{\rm cor}$ [29,31]:

$$E = \int d\boldsymbol{r}[H_{\rm kin} + H_{\rm Sky} + H_C] + H_{\rm Pair} + E_{\rm cor}. \quad (1)$$

The correction term in Eq. (1) approximately cancels the energy of spurious center-of-mass motion due to broken symmetries. The kinetic, nuclear and Coulomb energy density functionals read [29,30,32]

$$H_{\rm kin} = \frac{\hbar^2}{2m}\sum_{i=n,p}\tau_i(\rho_i, \nabla\rho_i, \nabla^2\rho_i), \quad (2)$$

$$\begin{aligned} H_{\rm Sky} = {} & \frac{t_0}{2}\left[\left(1+\frac{x_0}{2}\right)\rho^2 - \left(x_0+\frac{1}{2}\right)\sum_{i=p,n}\rho_i^2\right] \\ & + \frac{1}{12}t_3\rho^\alpha\left[\left(1+\frac{x_3}{2}\right)\rho^2 - \left(x_3+\frac{1}{2}\right)\sum_{i=p,n}\rho_i^2\right] \\ & + \frac{1}{4}\left[t_1\left(1+\frac{x_1}{2}\right) + t_2\left(1+\frac{x_2}{2}\right)\right]\rho\tau \\ & + \frac{1}{4}\left[t_2\left(x_2+\frac{1}{2}\right) - t_1\left(x_1+\frac{1}{2}\right)\right]\sum_{i=p,n}\rho_i\tau_i \\ & + \frac{1}{16}\left[3t_1\left(1+\frac{x_1}{2}\right) - t_2\left(1+\frac{x_2}{2}\right)\right](\nabla\rho)^2 \\ & - \frac{1}{16}\left[3t_1\left(x_1+\frac{1}{2}\right) + t_2\left(x_2+\frac{1}{2}\right)\right]\sum_{i=p,n}(\nabla\rho_i)^2 \\ & + \frac{W_0}{2}\left(\boldsymbol{J}\cdot\nabla\rho + \sum_{i=p,n}\boldsymbol{J_i}\cdot\nabla\rho_i\right) \\ & + \frac{1}{16}\left[(t_1-t_2)\sum_{i=p,n}\boldsymbol{J}_i^2 - (t_1x_1+t_2x_2)\boldsymbol{J}^2\right], \end{aligned} \quad (3)$$

and

$$H_C = \frac{e^2}{2}\rho_p(\boldsymbol{r})\int\frac{\rho_p(\boldsymbol{r'})}{|\boldsymbol{r}-\boldsymbol{r'}|}d\boldsymbol{r'} - \frac{3e^2}{4}\left(\frac{3}{\pi}\right)^{1/3}[\rho_p(\boldsymbol{r})]^{4/3}. \quad (4)$$

Here, ρ_i $(i = p, n)$ represent the protons' (p) and neutrons' (n) local density, while τ_i and $\boldsymbol{J_i}$, respectively, define the kinetic energy and the spin-orbit densities of protons and neutrons ($\rho = \rho_p + \rho_n$ and $\tau = \tau_p + \tau_n$). These densities are determined in terms of single-particle wave functions as the sums over the single-particle occupied states [30,33]. The Skyrme energy functional (3) consists of zero- and finite-range, effective-mass, and density-dependent contributions, in addition to the spin-orbit and tensor couplings [33]. In the present work, we consider the SLy4 parametrization of

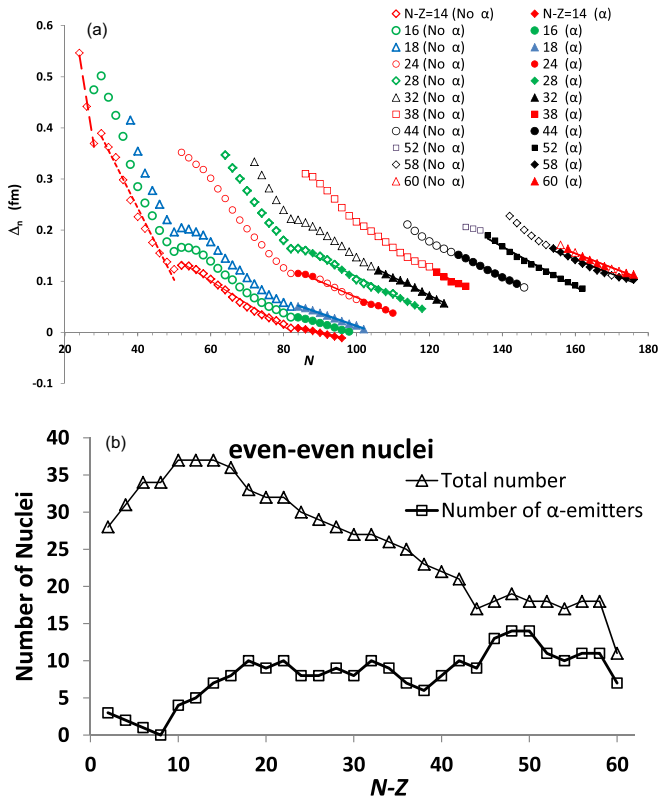

FIG. 2. (a) The neutron-skin thickness as a function of N for various indicated isospin-asymmetry chains. (b) Total number of known even-even nuclei belonging to different $N-Z$ chains with $N-Z$ from 2 to 60, and the number of α emitters among them.

the Skyrme force with the parameters ($x_{0,1,2,3}$, $t_{1,2,3}$, α, W_0) [33]. This SLy4 parametrization effectively allows us to describe well the nuclear structure and nuclear matter properties [18,34–37]. It is also widely used in the nuclear reactions [19,38–40] and neutron stars [41,42] studies, and in the investigation of the α and cluster decays of heavy nuclei [13,20,43,44]. While the first term in Eq. (4) gives the direct part of the Coulomb energy, the second term accounts for its exchange parts in the Slater approximation [45]. The pairing energy functional is added in Eq. (1) with the constant pairing matrix elements G_i as

$$H_{\rm Pair} = -\sum_{i=p,n} G_i \left[\sum_{\beta_i} \sqrt{n_{\beta_i}(1-n_{\beta_i})}\right]^2. \tag{5}$$

The BCS occupation numbers n_β are given in terms of pairing gap δ_i and Fermi energy ϵ_{Fi} as

$$n_{\beta_i} = \frac{1}{2}\left[1 - \frac{\epsilon_{\beta_i} - \epsilon_{Fi}}{\sqrt{(\epsilon_{\beta_i} - \epsilon_{Fi})^2 + \delta_i^2}}\right]. \tag{6}$$

In the constant force treatment of pairing, δ_i and ϵ_{Fi} are simultaneously determined by the gap equation $\delta_i/G_i = \sum_{\beta_i}\sqrt{n_{\beta_i}[1-n_{\beta_i}]}$ and the particle number $N_i = \sum_{\beta_i} n_{\beta_i}$ condition. Also, the pairing gap might be directly parametrized in the constant-gap approximation [29]. To obtain the nucleon-density profiles, we perform the calculations using the code of Ref. [46]. The local proton and neutron densities are obtained by the single-particle wave functions $\varphi^l(\boldsymbol{r},\sigma)$ and the occupation numbers n_{β_i} in terms of the orbital l and spin σ quantum numbers $\beta = (l,\sigma)$ as a sum over the single-particle occupied states [30,33],

$$\rho_{i=p(n)}(\boldsymbol{r}) = \sum_{\beta_i} \left|\varphi_i^l(\boldsymbol{r},\sigma)\right|^2 n_{\beta_i}. \tag{7}$$

The kinetic (τ_i) and the spin-orbit ($\boldsymbol{J}_i$) densities are obtained similarly as

$$\tau_i(\boldsymbol{r}) = \sum_{\beta_i} \left|\nabla\varphi_i^l(\boldsymbol{r},\sigma)\right|^2 n_{\beta_i}, \tag{8}$$

and

$$\boldsymbol{J}_i(\boldsymbol{r}) = \sum_{\beta_i(l,\sigma),\sigma'} \varphi_i^{l*}(\boldsymbol{r},\sigma')\nabla\varphi_i^l(\boldsymbol{r},\sigma)\times\langle\sigma'|\boldsymbol{\sigma}|\sigma\rangle n_{\beta_i}. \tag{9}$$

For stationary ground-state of spherical nuclei, we can separate the single-particle wave function in terms of its radial part $R_{l,\sigma}$ and the spinor spherical harmonics $Y_{j_{l,\sigma}\ell_{l,\sigma}}$ [46],

$$\varphi_{l,\sigma}(\boldsymbol{r}) = \frac{R_{l,\sigma}}{r} Y_{j_{l,\sigma}\ell_{l,\sigma}}(\theta,\phi).$$

In this case, $R_{l,\sigma}$ and the local (ρ_i), kinetic (τ_i), and spin-orbit ($\boldsymbol{J}_i$) densities and fields can be radially represented, on an equidistant radial grid. The Hartree-Fock equations for $R_{l,\sigma}$ can be found by varying the energy functional relative to $R_{l,\sigma}$, with the constraint that $R_{l,\sigma}$ are orthonormal. The obtained single-particle wave functions describe the many-body state as a Slater determinant given by the antisymmetrized product of occupied single-particle states. While a pure Slater state is reasonable for doubly magic nuclei, high density of degenerate states in the nuclei of partially open shells allows the residual two-body interaction to mix these states, to find a unique ground state [47] with the help of the used nuclear pairing scheme [48]. A careful treatment should be employed to evaluate the second derivative for the inversion of the mean-field Hamiltonian, with regard to the inverse gradient step. The pairing equations can be solved iteratively by using Newton's tangential method to satisfy the particle-number condition $N_i = \sum_{\beta\in i}\omega_\beta$ for a given group of single-particle energies ϵ_β. After obtaining the self-consistent solution of the SHFB equations using the considered density functionals with pairing, we can explicitly evaluate the single-particle wave functions, the corresponding single-particle energies, and the total energy of the system. The SHFB equations can be solved either by the two-basis method [49] with diagonalizing the particle-particle part of the Hamiltonian considering box boundary conditions, or by the canonical-basis method with spatially localized eigenstates of the one-body density matrix far away from the quasiparticle representation [50,51].

The root mean square radii of the proton and neutron distributions are obtained as

$$R_i^{rms} = \langle R_i^2\rangle^{1/2} = \left(\frac{\int r_i^2\rho_i(\boldsymbol{r})d\boldsymbol{r}}{\int\rho_i(\boldsymbol{r})d\boldsymbol{r}}\right)^{1/2}. \tag{10}$$

The neutron-skin thickness, which defines the extension of the neutron density distribution relative to the proton density, is

established in terms of the obtained *rms* radii as

$$\Delta_n = \langle R_n^2 \rangle^{1/2} - \langle R_p^2 \rangle^{1/2}. \quad (11)$$

The neutron-skin thickness directly addresses the isospin-asymmetry of nuclei associated with number of neutrons exceeding the proton number.

III. RESULTS AND DISCUSSION

Figure 2(a) shows the neutron-skin thickness for different nuclear $N-Z$ chains with even $N-Z$ from 14 to 60. The presented nuclei are distinguished according to their α radioactivity. While the solid symbols represent α emitters, the open symbols represent stable nuclei against α emission. As found, all the even-even α emitters with $N-Z \leqslant 12$ have a proton skin instead of neutron skin. For the nuclei of $(N-Z)$-chain, the heavier nuclei exhibit less neutron-skin thickness and tend to emit α particles [Fig. 2(a)], producing daughter nuclei with larger Δ_n. The larger the value of Δ_n, the larger the stability against α emission. The α emission is accompanied by less increase of Δ_n from parent to daughter nuclei than the corresponding increase of Δ_n from (Z,N) nucleus to $(Z-2,N-2)$ nucleus if there is no α emission. As seen, Δ_n varies along the $N-Z=14$ chain with four different rates. The α emitters show the smallest increase rate of Δ_n from (Z,N) to $(Z-2,N-2)$ nuclei. The steepness of this increase is larger for the successive nuclei which do not show α emission. This rate increases for the nuclei with $50 < N \leqslant 82$ and increases even more for the $28 < N \leqslant 50$ nuclei. The steepest increase of Δ_n with decreasing N is assigned to the light nuclei with $N \leqslant 28$. The α emitters belonging to different chains always exhibit the less increasing rate of Δ_n, from parent to daughter nuclei, except for the $N-Z=50$ chain in which the $(Z-2,N-2)$ nucleus approaches $N=126$ and demonstrates small change of Δ_n with respect to the (Z,N) nucleus.

Figure 2(b) displays the total number of the known even-even nuclei of different $N-Z$ chains with $N-Z$ from 2 to 60, and the number of α emitters among them. At $N-Z>8$, the number of nuclei generally decreases with increasing isospin asymmetry $N-Z$. For the $N-Z$ chains with $N-Z \leqslant 40$, the share of α emitters does not exceed 37% (10 nuclei). Only one even-even α emitter is observed for the chain with $N-Z=6$(3%), while none is observed for the $N-Z=8$ chain. The share of α emitters significantly increases at $N-Z=42$, reaching a maximum value of about 78% (14 α emitters) for the distinctive $N-Z=50$ chain. The number and share of α emitters decrease again for the chains with $N-Z>50$.

Regarding the isospin dependence of Δ_n, Fig. 3(a) shows the neutron-skin thickness of the nuclei belonging to the $N-Z$ chains displayed in Fig. 2(a) in addition to the $N-Z=2$ and 10 chains, as a function of the isospin symmetry parameter $I=(N-Z)/A$. The nuclei are grouped in different panels of Fig. 3(a) according to the neutron and proton shell closures. Namely, a group of incomplete proton shells with $Z_0=50$, two groups with extra protons above $Z_0=50$ and 60, and three groups of extra protons and neutrons above $(Z_0,N_0)=(82,82)$, (82,126), and (82,150) are shown in Fig. 3(a). As

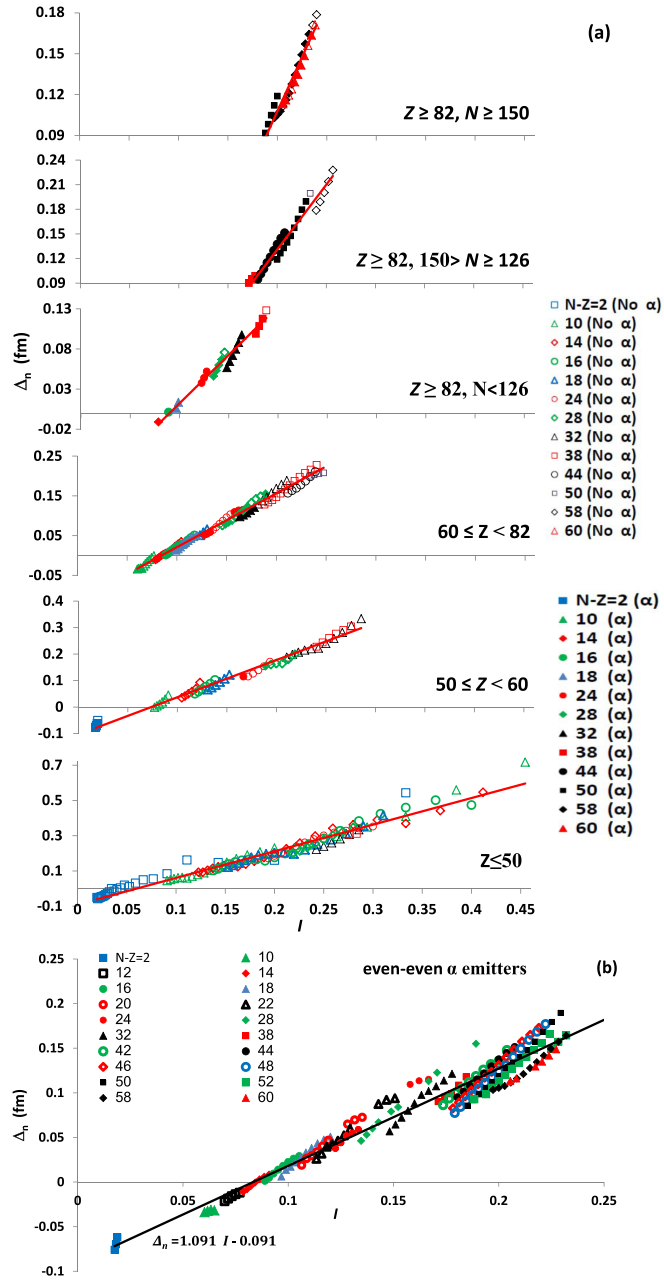

FIG. 3. (a) The neutron-skin thickness of even-even α emitters (solid symbols) and non α emitters (open symbols) in nuclei of $N-Z$ chains indicated as a function of I. The nuclei are grouped according their shell or subshell closures at $Z_0=50$, 60, and 82 and $N_0=126$ and 150. (b) The neutron-skin thickness of even-even α emitters as a function of I for the nuclei of the $N-Z$ chains indicated.

seen, in each group of nuclei the value of Δ_n depends almost linearly on I. All calculated Δ_n versus I for even-even α emitters are presented in Fig. 3(b). Regardless of the value of $N-Z$, the neutron-skin thicknesses are roughly aligned along the line

$$\Delta_n = 1.091I - 0.091. \quad (12)$$

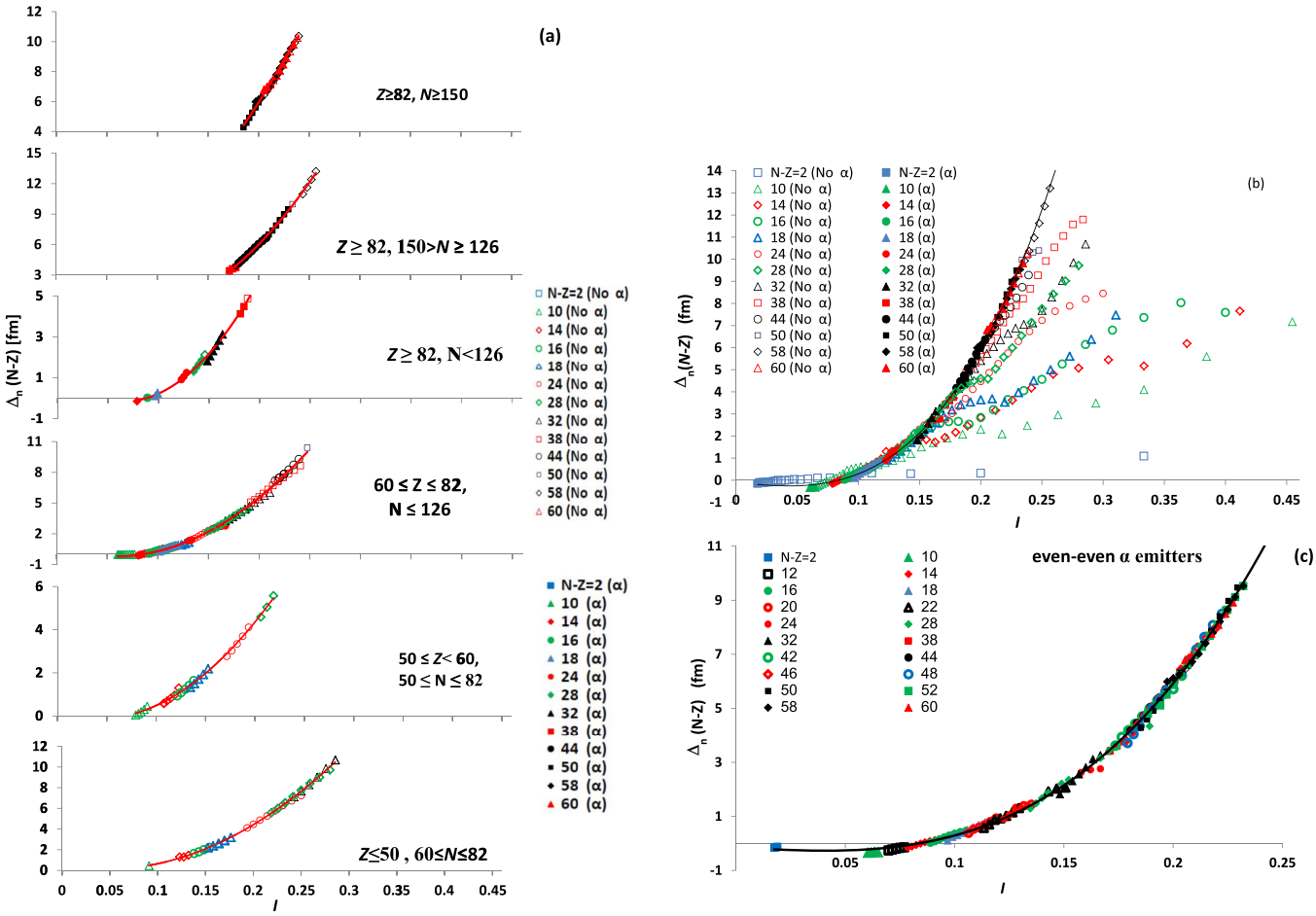

FIG. 4. (a) The dependencies of $\Delta_n(N-Z)$ on I for even-even nuclei belonging to the $N-Z$ chains indicated. The nuclei are grouped according their shell closures. The nuclei which emit and do not emit α particles are marked by close and open symbols, respectively. (b) The same as in panel (a), but for all even-even nuclei belonging to the indicated isospin chains. (c) The same as in panel (b), but only for even-even α emitters.

Sothe value of Δ_n depends approximately linearly on I. Even the nuclei with a proton-skin thickness ($\Delta_n < 0$) follows this trend. The corresponding Δ_n for the non α emitters [open symbols in Fig. 3(a)] considerably deviate from the line (12).

Figure 4(a) shows the products $\Delta_n(N-Z)$ as functions of the isospin asymmetry parameter I, for the same isospin chains as in Fig. 3(a). As seen, the symbols in each group lie on a parabola. If the values of $\Delta_n(N-Z)$ for all nuclei of various groups are displayed in one panel [Fig. 4(b)], we see that the $\Delta_n(N-Z)$ for even-even α emitters are maximal and well aligned along the parabolic curve

$$\Delta_n(N-Z) = 342I^2 - 44I + 1, \tag{13}$$

which is separately depicted in Fig. 4(c). The nuclei with proton-skin thickness ($\Delta_n < 0$) also correspond to Eq. (13). So, the value of Δ_n for an unknown α emitter can be estimated from Eq. (13). The neutron-skin thicknesses of non α emitters [the open symbols in Fig. 4(b)] substantially deviate from the curve defined by Eq. (13). Comparing Eqs. (12) and (13), we conclude the better parametrization of Δ_n with the latter expression.

Figure 5(a) shows the observed half-lives T_α against α decay as functions of $Q_\alpha^{-1/2}$ for even-even α emitters belonging to various isospin asymmetry $N-Z$ chains. As seen, the value of T_α exponentially increases with $Q_\alpha^{-1/2}$. However, the increase rates are different in each group of nuclei matching certain shell closures. This exponential relationship covers a wide range of half-lives, about 32 orders of magnitude.

To consider the dependence of T_α on neutron-skin thickness, we display in Figs. 5(b) and 5(c) the experimental T_α as a function of Δ_n for the isospin chains with $N-Z$ from 2 to 60. In Fig. 5(b), the results are presented for even-even nuclei with neutron and/or proton holes below the corresponding closed shells at N_0 and/or Z_0 ($N-N_0 < 0$ and/or $Z-Z_0 < 0$). For the nuclei with uncompleted shells, the half-lives increase with neutron-skin thickness. For example, there are nine even-even nuclei in the $N-Z=32$ chain with the measured values of T_α. The lightest nuclei ^{184}Os and ^{180}W of this isospin chain are more stable and have the largest neutron-skin thickness. Despite some deviations, T_α approximately depends exponentially on Δ_n in the isospin chain. The deviations can be related

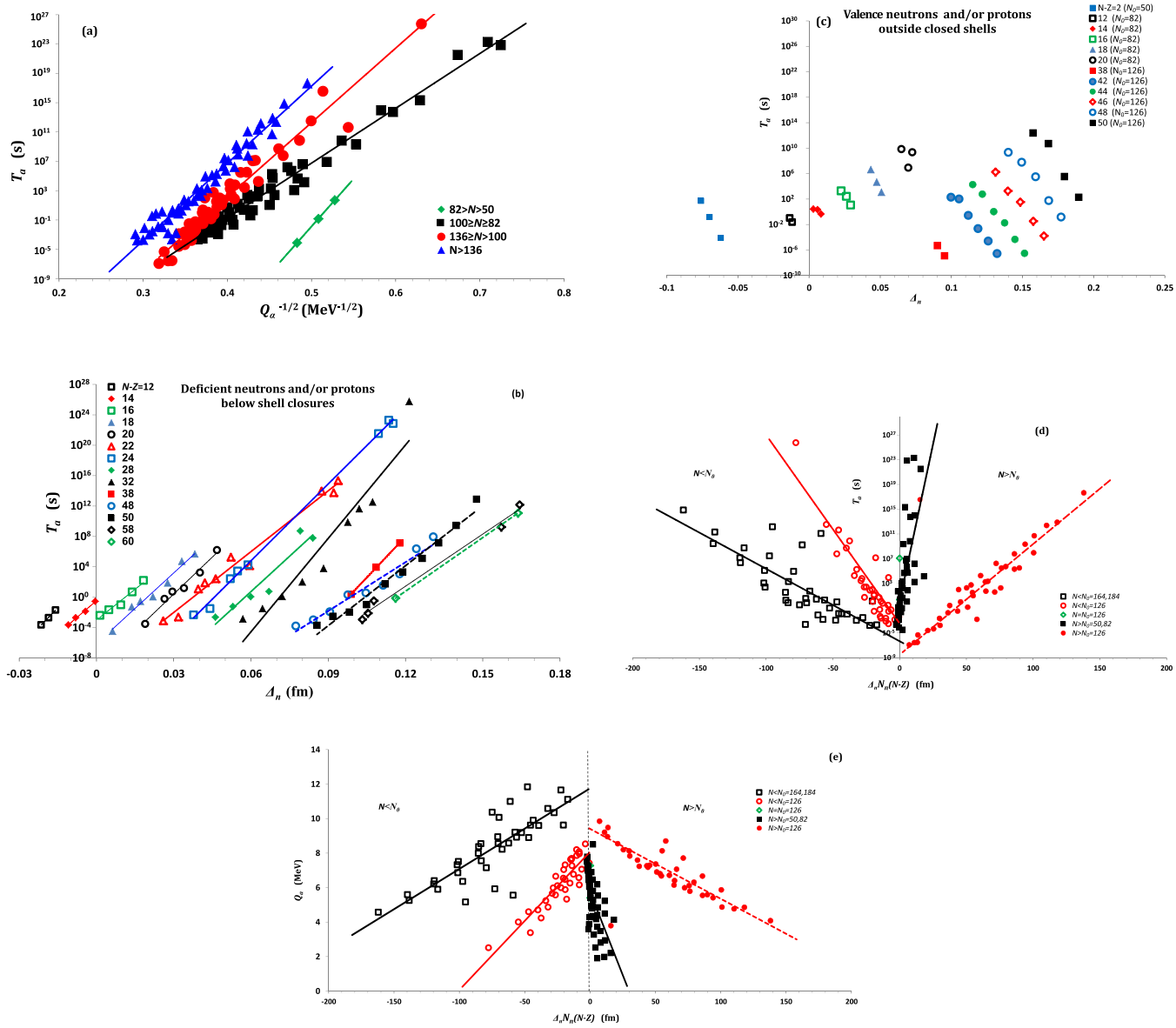

FIG. 5. (a) The observed α-decay half-lives versus $Q_\alpha^{-1/2}$ for even-even nuclei belonging to the isospin-asymmetry chains indicated. The nuclei are grouped according to their shell closure. (b) The observed α-decay half-lives versus Δ_n for the even-even nuclei with neutron and/or proton holes to complete closed shells (at N_0 and Z_0) The nuclei are grouped according to their isospin asymmetry. (c) The same as in panel (b), but for the nuclei with an excess of neutrons and/or protons outside closed shells. The nuclei are grouped according to their isospin asymmetry and closed shells. (d) The observed T_α and (e) corresponding Q_α values versus $\Delta_n N_n(N-Z)$ for even-even α emitters grouped according to their neutron shell closure (N_0).

to different single-particle levels of the nucleus that emitted the α particle. These peculiarities of nuclear structure are not taken into account in our consideration.

Figure 5(c) shows the data for nuclei with valent neutrons and/or protons outside closed shells ($N-N_0>0$ and/or $Z-Z_0>0$). As seen, the half-life against α decay for the nuclei of the isospin chain decreases with increasing Δ_n. T_α still shows an increasing trend with isospin asymmetry $(N-Z)$. For $N_0=126$, the six isospin asymmetry chains with $N-Z=38$, 42, 44, 46, 48, and 50 are depicted in Fig. 5(c). Even though T_α show a steadily decreasing behavior with increasing Δ_n, the irregularity in the rate of decrease can be related to different origins of nucleons forming the emitted α particle. While two neutrons forming the α particle emitted from ^{218}Po and ^{222}Ra probably come from the neutron orbital $\nu 2g_{9/2}$, those forming the α particle in ^{226}Rn and ^{230}Th come from the $\nu 1i_{11/2}$ orbital. The protons forming the α particles in these four nuclei are probably from the same $\pi 1h_{9/2}$ orbital.

In Figs. 5(d) and 5(e), we respectively display the observed α-decay half-lives [52] and corresponding Q_α values [53] as functions of isospin asymmetry $\Delta_n N_n(N-Z)$ for the even-even α emitters. The results for the nuclei with a number of neutrons between the given magic or semimagic numbers ($N_0=50$, 82, 126, 164, 184) are lined up along the lines indicated. The four sets of nuclei in Figs. 5(d) and 5(e) are distinguished by the excess number of neutrons outside the

$N_0 = 50$, 82, and 126 closed neutron shells, and the lack of neutrons to $N_0 = 126$ and 164, 184 neutron shell or subshell closures. The largest deviations of T_α from the corresponding lines are usually observed for nuclei with large uncertainty in the definition of the α-decay branching ratio [52]. Using the correlations found in Figs. 5(d) and 5(e), one can estimate T_α for currently unknown isotopes.

IV. SUMMARY

We found the correlations between the properties of α decay of even-even nuclei and their isospin asymmetry $N - Z$. The isospin-asymmetry chains with $N - Z$ from 2 to 60 were considered. In most cases, the α emitters exhibit smaller change of Δ_n from (Z, N) to $(Z - 2, N - 2)$ nuclei than the nuclei which do not emit α particles. The neutron-skin thicknesses Δ_n in α emitters are tightly aligned along a straight line as a function of isospin-asymmetry parameter I. Even the nuclei possessing a proton-skin thickness $(-\Delta_n)$ are closely aligned along this trendline. The values of $\Delta_n(N - Z)$ in the α emitters are closely aligned along a parabola as a function of I. Generally, the T_α tends to increase with isospin asymmetry $N - Z$, indicating relatively more stable nuclei against α decay. For the nuclei of incomplete closed shells of neutrons, the half-life against α decay increases with neutron-skin thickness. This can be understood in the context of the number of neutron holes to the next shell closure and in terms of the nucleon orbitals from which the nucleons forming α particles are coming. For the nuclei with valence neutrons and/or protons outside a magic core, the T_α in the nuclei of the same isospin chain decreases with increasing Δ_n. Distinct linear dependencies of both $\log_{10}(T_\alpha)$ and Q_α on $\Delta_n N_n(N - Z)$ are obtained for the corresponding closed neutron core. The correlation found can be used to estimate the values of T_α and Q_α if only the nucleon density profiles are calculated or measured.

ACKNOWLEDGMENTS

G.G.A. and N.V.A. were supported by Ministry of Science and Higher Education of the Russian Federation (Contract No. 075-10-2020-117). This work was supported in part by the RFBR (Moscow, 20-02-00176) and the ARE-JINR cooperation program.

[1] V. E. Viola, Jr. and G. T. Seaborg, J. Inorg. Nucl. Chem. **28**, 741 (1966).
[2] D. N. Poenaru and W. Greiner, J. Phys. G **17**, S443 (1991).
[3] R. G. Lovas, R. J. Liotta, A. Insolia, K. Varga, and D. S. Delion, Phys. Rep. **294**, 265 (1998).
[4] G. Royer, J. Phys. G **26**, 1149 (2000).
[5] A. Parkhomenko and A. Sobiczewski, Acta Phys. Pol. B **36**, 3095 (2005).
[6] Z. Ren, C. Xu, and Z. Wang, Phys. Rev. C **70**, 034304 (2004).
[7] D. Ni, Z. Ren, T. Dong, and C. Xu, Phys. Rev. C **78**, 044310 (2008).
[8] D. N. Poenaru, R. A. Gherghescu, and W. Greiner, Phys. Rev. C **83**, 014601 (2011).
[9] A. Zdeb, M. Warda, and K. Pomorski, Phys. Rev. C **87**, 024308 (2013).
[10] M. Ismail, W. M. Seif, A. Y. Ellithi, and A. Abdurrahman, Phys. Rev. C **92**, 014311 (2015).
[11] D. N. Poenaru, Y. Nagame, R. A. Gherghescu, and W. Greiner, Phys. Rev. C **65**, 054308 (2002).
[12] S. N. Kuklin, G. G. Adamian, and N. V. Antonenko, Phys. Rev. C **71**, 014301 (2005).
[13] W. M. Seif, Phys. Rev. C **91**, 014322 (2015); J. Phys. G: Nucl. Part. Phys. **40**, 105102 (2013).
[14] C. Xu, Z. Ren, and J. Liu, Phys. Rev. C **90**, 064310 (2014).
[15] J. Dong, W. Zuo, and J. Gu, Phys. Rev. C **87**, 014303 (2013).
[16] E. Shin, Y. Lim, C. H. Hyun, and Y. Oh, Phys. Rev. C **94**, 024320 (2016).
[17] Y. L. Zhang and Y. Z. Wang, Phys. Rev. C **97**, 014318 (2018).
[18] W. M. Seif, Hisham Anwer, and A. R. Abdulghany, Ann. Phys. (NY) **401**, 149 (2019).
[19] W. M. Seif, Eur. Phys. J. A **38**, 85 (2008).
[20] W. M. Seif, N. V. Antonenko, G. G. Adamian, and H. Anwer, Phys. Rev. C **96**, 054328 (2017).
[21] F. Minato and K. Hagino, Phys. Rev. C **77**, 044308 (2008).
[22] W. M. Seif, M. Shalaby, and M. F. Alrakshy, Phys. Rev. C **84**, 064608 (2011).
[23] C. Kim, A. K. Leibovich, and T. Mehen, Phys. Rev. D **78**, 054024 (2008).
[24] W. M. Seif, A. R. Abdulghany, and Z. N. Hussein, J. Phys. G **48**, 025111 (2021).
[25] S. Raman, C. W. Nestor, and P. Tikkanen, At. Data Nucl. Data Tables **78**, 1 (2001).
[26] D. T. Akrawy, H. Hassanabadi, S. S. Hosseini, and K. P. Santhosh, Nucl. Phys. A **975**, 19 (2018).
[27] B. A. Gheshlagh and O. N. Ghodsi, Chin. Phys. C **43**, 124105 (2019).
[28] J.-G. Deng, J.-C. Zhao, D. Xiang, and X.-H. Li, Phys. Rev. C **96**, 024318 (2017).
[29] J. R. Stone and P.-G. Reinhard, Prog. Part. Nucl. Phys. **58**, 587 (2007).
[30] J. W. Negele and D. Vautherin, Phys. Rev. C **5**, 1472 (1972).
[31] R. Jodon, M. Bender, K. Bennaceur, and J. Meyer, Phys. Rev. C **94**, 024335 (2016).
[32] E. Chabanat, E. Bonche, E. Haensel, J. Meyer, and R. Schaeffer, Nucl. Phys. A **627**, 710 (1997).
[33] E. Chabanat, E. Bonche, E. Haensel, J. Meyer, and R. Schaeffer, Nucl. Phys. A **635**, 231 (1998).
[34] L. Bonneau, P. Quentin, and K. Sieja, Phys. Rev. C **76**, 014304 (2007).
[35] A. S. Umar and V. E. Oberacker, Phys. Rev. C **76**, 024316 (2007).
[36] W. M. Seif and H. Mansour, Int. J. Mod. Phys. E **24**, 1550083 (2015).
[37] A. P. Severyukhin, S. Åberg, N. N. Arsenyev, and R. G. Nazmitdinov, Phys. Rev. C **95**, 061305(R) (2017).
[38] Z.-Q. Feng, G.-M. Jin, and F.-S. Zhang, Nucl. Phys. A **802**, 91 (2008).
[39] R. Keser, A. S. Umar, and V. E. Oberacker, Phys. Rev. C **85**, 044606 (2012).

[40] W. M. Seif, A. I. Refaie, and M. M. Botros, Indian J. Phys. **92**, 393 (2018).
[41] N. Chamel, S. Goriely, and J. M. Pearson, Phys. Rev. C **80**, 065804 (2009).
[42] J. R. Stone, J. C. Miller, R. Koncewicz, P. D. Stevenson, and M. R. Strayer, Phys. Rev. C **68**, 034324 (2003).
[43] D. E. Ward, B. G. Carlsson, and S. Åberg, Phys. Rev. C **88**, 064316 (2013).
[44] W. M. Seif, M. M. Botros, and A. I. Refaie, Phys. Rev. C **92**, 044302 (2015).
[45] C. Titin-Schnaider and P. H. Quentin, Phys. Lett. B **49**, 213 (1974).
[46] P.-G. Reinhard, in *Computational Nuclear Physics*, edited by K. Langanke, J. A. Maruhn, and S. E. Koonin (Springer-Verlag, Berlin, 1990), Vol. 1, Chap. 2.
[47] P.-G. Reinhard and E. W. Otten, Nucl. Phys. A **420**, 173 (1984).
[48] M. Bender, P.-H. Heenen, and P.-G. Reinhard, Rev. Mod. Phys. **75**, 121 (2003).
[49] J. Terasaki, H. Flocard, P.-H. Heenen, and P. Bonche, Nucl. Phys. A **621**, 706 (1997).
[50] P.-G. Reinhard, M. Bender, K. Rutz, and J. A. Maruhn, Z. Phys. A: Hadrons Nucl. **358**, 277 (1997).
[51] M. V. Stoitsov, J. Dobaczewski, W. Nazarewicz, and P. Ring, Comput. Phys. Commun. **167**, 43 (2005).
[52] G. Audi, F. G. Kondev, Meng Wang, W. J. Huang, and S. Naimi, Chin. Phys. C **41**, 030001 (2017).
[53] M. Wang, G. Audi, F. G. Kondev, W. J. Huang, S. Naimi, and X. Xu, Chin. Phys. C **41**, 030003 (2017).